Kinetics of Electron Transfer through the Respiratory Chain

Qusheng Jin and Craig M. Bethke
Department of Geology, University of Illinois, Urbana, Illinois 61801-2919 USA

ABSTRACT We show that the rate at which electrons pass through the respiratory chain in mitochondria and respiring prokaryotic cells is described by the product of three terms, one describing electron donation, one acceptance, and a third, the thermodynamic drive. We apply the theory of nonequilibrium thermodynamics in the context of the chemiosmotic model of proton translocation and energy conservation. This approach leads to a closed-form expression that predicts steady-state electron flux as a function of chemical conditions and the proton motive force across the mitochondrial inner membrane or prokaryotic cytoplasmic membrane. The rate expression, derived considering reverse and forward electron flow, is the first to account for both thermodynamic and kinetic controls on the respiration rate. The expression can be simplified under specific conditions to give rate laws of various forms familiar in cellular physiology and microbial ecology. The expression explains the nonlinear dependence of flux on electrical potential gradient, its hyperbolic dependence on substrate concentration, and the inhibiting effects of reaction products. It provides a theoretical basis for investigating life under unusual conditions, such as microbial respiration in alkaline waters.

INTRODUCTION

The respiratory electron transport chain in the inner membrane of mitochondria and cytoplasmic membrane of many bacteria conserves energy derived from redox reactions into a proton motive force (Δp, or PMF) across the membrane (Mitchell, 1961, 1968). The cell uses the PMF to drive critical reactions, such as synthesizing ATP from ADP and transporting substrates. Given the central role of the transport chain to cellular metabolism, developing a quantitative description of electron flux through the chain is of fundamental importance to understanding life processes in respiring organisms.

Most approaches to this problem, such as the linear nonequilibrium thermodynamic model (Rottenberg, 1973, 1979; Caplan and Essig, 1983; Westerhoff and van Dam, 1987) and metabolic control analysis (Groen et al., 1982; Brown, 1992; Fell, 1992; Moreno-Sánchez et al., 1999), have not accounted for the internal function of the respiratory chain or the mechanism of energy conservation, and hence yield limited insight to the controls on the rate of electron transfer in a cell. Structured models (Wilson et al., 1977, 1979; Rohde and Reich, 1980; Bohnensack, 1981; Holzhütter et al., 1985; Korzeniewski and Froncisz, 1991; Korzeniewski and Mazat, 1996; Cristina and Hernández, 2000), in contrast, are tied closely to the internal mechanism of the transport chain, but are sufficiently complex to require solution by numerical simulation.

In this paper, on the basis of the metabolic pathways of electron transfer (Mitchell, 1961, 1966) and nonlinear nonequilibrium thermodynamics, we derive a closed-form expression that gives the steady-state flux of electrons through the transport chain. Under specific conditions, this expression can be simplified into rate laws of various familiar forms. We show that this expression predicts salient observations from experimental studies and provides new insight to the functioning of the respiratory chain.

CONCEPTUAL MODEL

According to chemiosmotic theory (Mitchell, 1961, 1966), the electron transport chain conserves into PMF the energy released when electrons are transferred from a donating half-reaction to an accepting half-reaction. The electrons pass through the respiratory chain, which is composed of a series of membrane-associated redox complexes (enzymes) and electron carriers (coenzymes). Details of the respiratory chain in mitochondria and bacteria differ among organisms and are subject to cell regulation (Richardson, 2000), but the overall mechanism is the same.

In our conceptual model (Fig. 1), the respiratory chain is composed of redox complexes and electron carriers. The overall chemical reaction driving electrons through the chain is

$$\sum_{\mathrm{D}} \nu_{\mathrm{D}}\mathrm{D} + \sum_{\mathrm{A}} \nu_{\mathrm{A}}\mathrm{A} \rightleftharpoons \sum_{\mathrm{D}^+} \nu_{\mathrm{D}^+}\mathrm{D}^+ + \sum_{\mathrm{A}^-} \nu_{\mathrm{A}^-}\mathrm{A}^-. \quad (1)$$

Here, D and D^+ represent the species on the reduced and oxidized sides of the primary electron-donating half-reaction, A and A^- are the species on the oxidized and reduced sides of the terminal-accepting half-reaction, and ν_D, etc., are the reaction coefficients. Reaction 1 drives the translocation of protons inside (H^+_{in}) to outside (H^+_{out}) the mem-

Submitted September 22, 2001, and accepted for publication May 7, 2002.

Address reprint requests to Q. Jin, Department of Geology, University of Illinois, 1301 W. Green St., 245 Natural History Bldg., Urbana, IL 61801-2919. Tel.: 217-244-8337; Fax: 217-244-4996; E-mail: qjin@aquifer.geology.uiuc.edu.

0006-3495/02/10/1797/12 $2.00

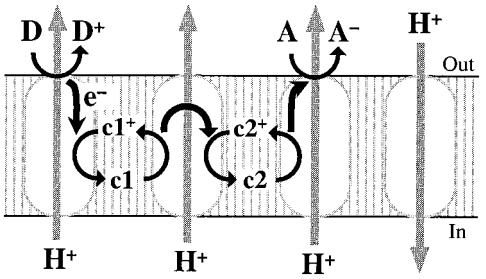

FIGURE 1 Generalized model of the electron transport chain within the membrane of a mitochondrion or respiring bacterium, showing resultant proton translocation. Electron(s) derived from a donating species D are transferred through the chain containing coenzymes c1 and c2 to an accepting species A. Reaction centers (ovals) are, from left to right: primary reductase, coenzyme reductase, terminal reductase, and a proton-translocating enzyme, such as ATP synthase.

brane, producing PMF. Adding this process to Reaction 1 gives the electrogenic redox reaction,

$$\sum_{\mathrm{D}} \nu_{\mathrm{D}}\mathrm{D} + \sum_{\mathrm{A}} \nu_{\mathrm{A}}\mathrm{A} + m\mathrm{H}^+_{\mathrm{in}} \rightleftharpoons \sum_{\mathrm{D}^+} \nu_{\mathrm{D}^+}\mathrm{D}^+ + \sum_{\mathrm{A}^-} \nu_{\mathrm{A}^-}\mathrm{A}^- + m\mathrm{H}^+_{\mathrm{out}}, \quad (2)$$

representing cell respiration. Here, m is the number of protons translocated outside of the membrane per unit turnover of the reaction. The reaction is termed electrogenic because it drives charged species across an electrical potential gradient. If n electrons are transferred per turnover of Reaction 2, the electron flux through the electrogenic reaction is given as

$$\nu = -\frac{n}{\nu_{\mathrm{D}}}\frac{\mathrm{d}[\mathrm{D}]}{\mathrm{d}t} = -\frac{n}{\nu_{\mathrm{A}}}\frac{\mathrm{d}[\mathrm{A}]}{\mathrm{d}t} = \frac{n}{\nu_{\mathrm{D}^+}}\frac{\mathrm{d}[\mathrm{D}^+]}{\mathrm{d}t} = \frac{n}{\nu_{\mathrm{A}^-}}\frac{\mathrm{d}[\mathrm{A}^-]}{\mathrm{d}t}, \quad (3)$$

where [D], [A], etc., represent species concentrations, and t is time.

Reaction 2 is composed of three steps, each of which involves a number of elementary chemical reactions catalyzed by one or more redox complexes. The three steps are electron donation (step D), electron transfer (step T), and electron acceptance (step A). In step D, electrons from the primary donating species are derived at the primary reductase and passed, perhaps through further redox complexes, to an arbitrary electron carrier in the chain, translocating m_{D} protons. The reaction proceeds according to

$$\sum_{\mathrm{D}} \nu_{\mathrm{D}}\mathrm{D} + \nu_{\mathrm{c1}}\mathrm{c1}^+ + m_{\mathrm{D}}\mathrm{H}^+_{\mathrm{in}} \rightleftharpoons \sum_{\mathrm{D}^+} \nu_{\mathrm{D}^+}\mathrm{D}^+ + \nu_{\mathrm{c1}}\mathrm{c1} + m_{\mathrm{D}}\mathrm{H}^+_{\mathrm{out}}, \quad (4)$$

where $\mathrm{c1}^+$ and c1 are the oxidized and reduced form of the carrier. In step T, the electrons pass to a second carrier, translocating a total of m_{T} protons,

$$\nu_{\mathrm{c1}}\mathrm{c1} + \nu_{\mathrm{c2}}\mathrm{c2}^+ + m_{\mathrm{T}}\mathrm{H}^+_{\mathrm{in}} \rightleftharpoons \nu_{\mathrm{c1}}\mathrm{c1}^+ + \nu_{\mathrm{c2}}\mathrm{c2} + m_{\mathrm{T}}\mathrm{H}^+_{\mathrm{out}}, \quad (5)$$

where $\mathrm{c2}^+$ and c2 are the carrier's oxidized and reduced forms. Step A passes electrons from the second electron carrier through the terminal reductase to the terminal electron-accepting species,

$$\sum_{\mathrm{A}} \nu_{\mathrm{A}}\mathrm{A} + \nu_{\mathrm{c2}}\mathrm{c2} + m_{\mathrm{A}}\mathrm{H}^+_{\mathrm{in}} \rightleftharpoons \sum_{\mathrm{A}^-} \nu_{\mathrm{A}^-}\mathrm{A}^- + \nu_{\mathrm{c2}}\mathrm{c2}^+ + m_{\mathrm{A}}\mathrm{H}^+_{\mathrm{out}}, \quad (6)$$

translocating m_{A} protons. The total number of translocated protons m is the sum of m_{D}, m_{T}, and m_{A}.

THERMODYNAMIC DRIVE

The thermodynamic drive for a chemical reaction is the reaction's affinity A, the free energy liberated per unit reaction progress (Price, 1998). The chemical affinity of a reaction (De Donder and Van Pysselberghe, 1936) is

$$A = -\sum_{\mathrm{i}} \nu_{\mathrm{i}}\mu_{\mathrm{i}}, \quad (7)$$

where μ_{i} is the electrochemical potential of each species i in the reaction. For an electrogenic redox reaction, μ_{i} is given,

$$\mu_{\mathrm{i}} = \mu^\circ_{\mathrm{i}} + RT\ln[i] + z_{\mathrm{i}}F\psi_{\mathrm{i}} \quad (8)$$

(Christensen, 1975). Here, μ°_{i} is the species' standard chemical potential, $[i]$ is its concentration (mol l^{-1}), and z_{i} is its electrical charge. Variable ψ_{i} is electrical potential at the species' location (inside or outside the membrane), R is the gas constant, T is absolute temperature, and F is Faraday's constant. For simplicity, we assume throughout this paper that species' activity coefficients are invariant and can be accommodated in the value of μ°_{i}.

From Eqs. 7 and 8, the affinity of Reaction 2 is

$$A = nF\Delta E - mF\Delta p, \quad (9)$$

where ΔE is the difference in redox potential between the donating and accepting half-reactions

$$\Delta E = \Delta E_{\mathrm{o}} - \frac{RT}{nF}\ln\frac{\prod_{\mathrm{D}^+}[\mathrm{D}^+]^{\nu_{\mathrm{D}^+}}\prod_{\mathrm{A}^-}[\mathrm{A}^-]^{\nu_{\mathrm{A}^-}}}{\prod_{\mathrm{D}}[\mathrm{D}]^{\nu_{\mathrm{D}}}\prod_{\mathrm{A}}[\mathrm{A}]^{\nu_{\mathrm{A}}}}. \quad (10)$$

Here, ΔE_{o} is the difference in the standard redox potentials between the reactions, calculated at the standard state of

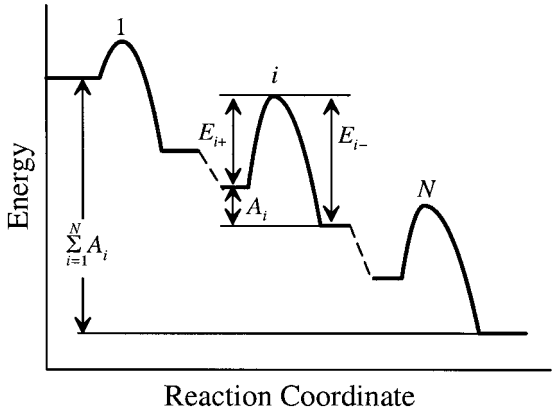

FIGURE 2 Variation with reaction progress of chemical energy for the overall electrogenic reaction. The electrogenic reaction is composed of N elementary reactions. Each elementary reaction i has a thermodynamic drive (or affinity) A_i, which is the difference between the forward and reverse activation energies, E_{i+} and E_{i-}.

interest, whether chemical or biological (i.e., $pH^o = 7$). The PMF Δp in Eq. 9,

$$\Delta p = \Delta\psi + \frac{RT}{F}\ln\frac{[H^+_{out}]}{[H^+_{in}]}, \tag{11}$$

depends on the difference $\Delta\psi$ between the electrical potential outside and inside the membrane ($\psi_{out} - \psi_{in}$), and the ratio across the membrane of proton concentration.

FORWARD AND REVERSE ELECTRON FLUXES

As is typical of enzyme-catalyzed reactions, the electron transport chain (including proton translocation) is composed of a series of elementary reactions that proceed forward and backward at the same time. For the ith elementary reaction in the series, according to Arrhenius's law, the forward and reverse fluxes v_{i+} and v_{i-} are given as

$$v_{i+} = C_i \exp\left(-\frac{E_{i+}}{RT}\right)$$

and

$$v_{i-} = C_i \exp\left(-\frac{E_{i-}}{RT}\right) \tag{12}$$

(Masel, 2001). Here, C_i is the pre-exponential constant, and E_{i+} and E_{i-} are the activation energies for forward and reverse reaction. The reaction's affinity A_i is the difference $E_{i-} - E_{i+}$ between activation energies, as can be seen in Fig. 2. The expression

$$\frac{v_{i+}}{v_{i-}} = \exp\left(\frac{A_i}{RT}\right) \tag{13}$$

then, gives the ratio of the forward to reverse fluxes.

For an overall reaction composed of N elementary reactions, Boudart (1976) showed that, at steady state, the ratio of the overall forward and reverse fluxes (ν_+ and ν_-) is given as

$$\frac{\nu_+}{\nu_-} = \prod_{i=1}^{N}\frac{v_{i+}}{v_{i-}}. \tag{14}$$

Expanding this relation, the equation

$$\frac{\nu_+}{\nu_-} = \exp\left(\sum_{i=1}^{N} A_i \Big/ RT\right) \tag{15}$$

gives the ratio of the overall fluxes.

The affinity A of the overall reaction, however, is not necessarily the sum of the affinities A_i of the elementary reactions because some of the elementary steps may occur in parallel. This phenomenon is accounted for in chemical kinetics by a quantity χ known as the average stoichiometric number (Temkin, 1963), defined as

$$\chi = A \Big/ \sum_{i=1}^{N} A_i. \tag{16}$$

The value of χ depends on how the thermodynamic drive is distributed over each individual elementary reaction, and how the overall reaction is written (how many electrons are transferred per unit turnover). Substituting Eq. 16 into 15,

$$\frac{\nu_+}{\nu_-} = \exp\left(\frac{A}{\chi RT}\right) \tag{17}$$

gives the relationship between the flux ratio and the thermodynamic drive (Horiuti, 1948; Hollingsworth, 1957); this equation constitutes an important tenet of irreversible thermodynamics.

The observed electron flux v through the electron transport chain is the difference between forward and reverse fluxes, so $v = \nu_+ - \nu_-$. Substituting into Eq. 17 gives the relation

$$v = \nu_+ F_T, \tag{18}$$

where

$$F_T = 1 - \exp\left(-\frac{A}{\chi RT}\right) \tag{19}$$

is the thermodynamic potential factor (TPF) (Happel, 1972). These relations show how, at steady state, the overall flux

depends on the thermodynamic drive (Boudart, 1976). The TPF can be written

$$F_T = 1 - \exp\left(-\frac{nF\Delta E - mF\Delta p}{\chi RT}\right) \quad (20)$$

by substituting Eq. 9 into 19. Alternatively, the TPF can be expanded by substituting Eq. 10 into the above equation,

$$F_T = 1 - \exp\left(\frac{-nF\Delta E^\circ + mF\Delta\psi}{\chi RT}\right) \times \left(\frac{[H^+_{out}]^m \prod_{D^+}[D^+]^{\nu_{D^+}} \prod_{A^-}[A^-]^{\nu_{A^-}}}{[H^+_{in}]^m \prod_D [D]^{\nu_D} \prod_A [A]^{\nu_A}}\right)^{1/\chi}, \quad (21)$$

which shows how concentrations of the species in the redox reaction and of the translocated protons affect thermodynamic drive.

Eq. 18 shows that, as the TPF increases toward its limiting value of unity, v at given chemical conditions (pH and concentrations of substrate and product species) approaches the value of v_+. As such, v_+ represents the flux capacity v_o, the greatest rate at which the respiratory chain can transfer electrons under given conditions.

RATE EXPRESSION

Electron transfer within the individual steps (D, T, and A) in the overall electrogenic reaction (Reaction 2), and the overall reaction itself, involves passage of electrons across one or more redox complexes; it includes intraprotein and interprotein transfer, and any resulting proton translocation. The process is too complex to describe directly using electron transfer theory (Davidson, 1996). Instead, a steady-state rate expression can be derived for the cases in which each of the steps A, T, and D consume most of the thermodynamic drive. Starting with the case for step T (Reaction 5), the thermodynamic drive consumed by steps D and A are taken to be small relative to the overall drive. In this case,

$$A_D = nF\Delta E^\circ_D - m_D F\Delta p - RT \ln \frac{[c1]^{\nu_{c1}} \prod_{D^+}[D^+]^{\nu_{D^+}}}{[c1^+]^{\nu_{c1}} \prod_D [D]^{\nu_D}} \simeq 0, \quad (22)$$

where A_D is the thermodynamic drive for step D.

The concentration ratio of carrier 1 in its reduced-to-oxidized forms, then, is

$$\frac{[c1]}{[c1^+]} = \frac{\prod_D [D]^{\beta_D}}{K_D \prod_{D^+}[D^+]^{\beta_{D^+}}}, \quad (23)$$

where

$$\beta_D = \frac{\nu_D}{\nu_{c1}} \quad \text{and} \quad \beta_{D^+} = \frac{\nu_{D^+}}{\nu_{c1}} \quad (24)$$

are stoichiometric coefficients; K_D is given as

$$K_D = \exp\left(-\frac{nF\Delta E^\circ_D - m_D F\Delta p}{\nu_{c1} RT}\right), \quad (25)$$

where ΔE°_D is the standard redox potential difference of Reaction 4.

The total concentration $[c1]_t$ of electron carrier 1 is the sum of [c1] and $[c1^+]$. We introduce a kinetic factor F_D

$$F_D = \frac{[c1]}{[c1]_t} = \frac{\prod_D [D]^{\beta_D}}{\prod_D [D]^{\beta_D} + K_D \prod_{D^+}[D^+]^{\beta_{D^+}}}, \quad (26)$$

which is the ratio in concentration of reduced-to-total carrier 1. This factor shows how the concentrations of species in the donating reaction affect the redox state of the electron carrier.

A second kinetic factor F_A is the concentration ratio of oxidized-to-total electron carrier 2,

$$F_A = \frac{[c2^+]}{[c2]_t} = \frac{\prod_A [A]^{\beta_A}}{\prod_A [A]^{\beta_A} + K_A \prod_{A^-}[A^-]^{\beta_{A^-}}}, \quad (27)$$

where the stoichiometric coefficients are

$$\beta_A = \frac{\nu_A}{\nu_{c2}} \quad \text{and} \quad \beta_{A^-} = \frac{\nu_{A^-}}{\nu_{c2}}. \quad (28)$$

K_A is given as

$$K_A = \exp\left(-\frac{nF\Delta E^\circ_A - m_A F\Delta p}{\nu_{c2} RT}\right), \quad (29)$$

where ΔE°_A is the standard redox potential difference of Reaction 6.

At steady state, each step (D, T, and A) in the overall electrogenic reaction proceeds at the net rate of the overall reaction (Kacser and Burns, 1979). The flux capacity for the overall reaction, then, is the capacity for step T, which can be written

$$v_o = k_+[E_T][c1][c2^+] \quad (30)$$

(Pring, 1969). Here, k_+ is the rate coefficient of step T, and E_T represents the redox complex that catalyzes the step. We can take the effective concentration $[E_T]$ of the redox complex at steady state to be proportional to [X], the total concentration of mitochondrial protein or bacterial biomass; we carry the ratio $[E_T]/[X]$ as ξ_T.

TABLE 1 Commonly used rate expressions for electron transfer through respiratory chain

	F_D	F_A	F_T
Saturation (or Monod) equation*			
$v = v_{max}\left(\frac{[D]}{K_D + [D]}\right)$	Constant $[D^+]$	1	1
$v = v_{max}\left(\frac{[A]}{K_A + [A]}\right)$	1	Constant $[A^-]$	1
Dual Monod equation†			
$v = v_{max}\left(\frac{[D]}{K_D + [D]}\right)\left(\frac{[A]}{K_A + [A]}\right)$	Constant $[D^+]$	Constant $[A^-]$	1
Linear equation‡			
$v = L \times A \quad L = v_{max}/\chi RT$	1	1	$\frac{A}{\chi RT} \rightarrow 0$
Hill's equation§			
$v = v_{max}[1 - \exp(-A/RT)]$	1	1	$\chi = 1$

*E.g., Gnaiger et al. (1995) and Monod (1949).
†Bae and Rittmann (1996).
‡Caplan (1983).
§Hill (1977).

Rearranging Eqs. 26 and 27, we can express [c1] and $[c2^+]$ in terms of F_D and F_A. Now, the flux capacity is

$$v_o = v_{max} F_D F_A, \tag{31}$$

where

$$v_{max} = k_o[X] \tag{32}$$

and

$$k_o = k_+ \xi_T [c1]_t [c2]_t. \tag{33}$$

Combining Eqs. 18 and 31, and remembering that v_+ is equal to v_o, the net electron flux can be seen to be the product of the kinetic factors (given by Eqs. 26 and 27) and the TPF,

$$v = v_{max} F_D F_A F_T. \tag{34}$$

F_T can be determined by the overall thermodynamic drive using Eq. 19, because step T consumes most of the overall thermodynamic drive.

In Eq. 34, the terms F_D and F_A represent the kinetic effects on the electron flux attributable to the donating and accepting reactions, respectively, and F_T reflects the thermodynamic control. The variable v_{max} represents the rate at which the respiratory chain transfers electrons under optimal conditions. The individual terms (K_D, K_A, v_{max}) required to evaluate this expression could in principle be determined from the parameters in Eqs. 25, 29, 32, and 33. In practice, they are likely to be determined empirically, by fitting the rate expression to experimental observations, as are the reaction orders β_D, etc. In the Appendix, we derive parallel rate expressions for the cases in which the electron donating step (D) and accepting step (A) consume most of the thermodynamic drive.

DISCUSSION

Relation to existing models

The rate expression (Eq. 34) we derived is a general relationship giving the electron flux through the respiratory chain under varying chemical conditions, for an arbitrary combination of donating and accepting reactions. We do not derive our equation in the statistical sense, in which we would work to find the minimum number of parameters that can be regressed to explain a given experiment data set. Instead, we derive our rate expression on the basis of a generalized pathway of electron transfer through the respiratory chain and nonlinear nonequilibrium thermodynamics. In this way, we identify the set of parameters that actually controls the system. Each factor considered in the conceptual model is accounted in our rate expression, even if only a subset of them is required to explain a given experiment data set. We cannot construct a quantitative model with fewer parameters without sacrificing generality.

Because of its generality, the rate expression (Eq. 34) is far more complicated in form than necessary to describe a specific application. Most experimental studies in bioenergetics are conducted under relatively stable conditions, where some chemical species remain invariant in concentration, or the overall electrogenic reaction remains close to, or far from, equilibrium. In practice, a number of models, such as the saturation equation, linear equation, and so on, have been suggested and applied in biophysics, as summarized in Table 1. None of these expressions accounts for both thermodynamic and kinetic effects (Gnaiger et al., 1995), however, and so none is fully general. Instead, the

existing models correspond to specific simplifications of the form of our rate expression (Fig. 3).

To demonstrate how the general expression can, under specific conditions, be simplified to give familiar rate laws, we consider electron transfer between succinate and NAD^+,

$$Suc^{2-} + NAD^+ + 4H^+_{out} \rightarrow Fum^{2-} + NADH + H^+ + 4H^+_{in} \quad (35)$$

(Suc^{2-} and Fum^{2-} are succinate and fumarate). By this reaction, electrons flow backward through the transport chain to conserve reducing power as NADH. Two electrons ($n = 2$) pass from succinate to redox complex II, quinones, and complex I, before being taken up by NAD^+. The energy to drive the reaction is obtained at complex I by translocating four protons inside the membrane ($m = -4$). The average stoichiometric number χ is an intrinsic property of the transport chain in a given configuration. The value of χ can be deduced from the shape of the curve representing electron flux versus thermodynamic drive, as shown in Fig. 3. We will show below (Fig. 4) that, for Reaction 35 in mitochondria, the value of χ is ~4.

Substituting n and m into Eq. 20, the TPF for this reaction is

$$F_T = 1 - \exp\left(-\frac{2F\Delta E + 4F\Delta p}{\chi RT}\right). \quad (36)$$

Taking the cytoplasmic pH to be constant, which fixes $[H^+_{in}]$, F_D and F_A can be written as

$$F_D = \frac{[Suc^{2-}]^{\beta_D}}{[Suc^{2-}]^{\beta_D} + K_D[Fum^{2-}]^{\beta_{D'}}}, \quad (37)$$

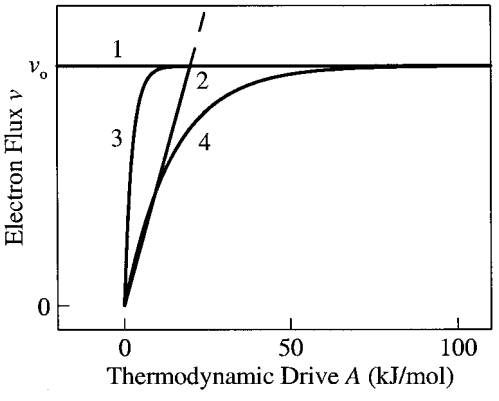

FIGURE 3 Descriptions of the thermodynamic control on electron flux v through the transport chain. The flux capacity v_o is the maximum electron flux under given chemical conditions. Lines represent: *1*, independent flux; *2*, linear nonequilibrium thermodynamic model; *3*, Hill's equation; and *4*, our analysis (TPF, Eq. 20), taking for this illustration a value of 4 for the average stoichiometric number χ.

$$F_A = \frac{[NAD^+]^{\beta_A}}{[NAD^+]^{\beta_A} + K_A[NADH]^{\beta_{A'}}}. \quad (38)$$

Now, the electron flux is given by the expression

$$v = v_{max}\left(\frac{[Suc^{2-}]^{\beta_D}}{[Suc^{2-}]^{\beta_D} + K_D[Fum^{2-}]^{\beta_{D'}}}\right) \times \left(\frac{[NAD^+]^{\beta_A}}{[NAD^+]^{\beta_A} + K_A[NADH]^{\beta_{A'}}}\right) \times \left[1 - \exp\left(-\frac{2F\Delta E + 4F\Delta p}{\chi RT}\right)\right], \quad (39)$$

which is clearly more manageable than the general rate law (Eq. 34).

Where Reaction 35 is far from equilibrium, the thermodynamic drive is large (i.e., $A \gg \chi RT$) and the TPF approaches one. In this case, the electron flux equals the flux capacity, and the rate expression (Eq. 39) becomes

$$v = v_{max}\left(\frac{[Suc^{2-}]^{\beta_D}}{[Suc^{2-}]^{\beta_D} + K_D[Fum^{2-}]^{\beta_{D'}}}\right) \times \left(\frac{[NAD^+]^{\beta_A}}{[NAD^+]^{\beta_A} + K_A[NADH]^{\beta_{A'}}}\right). \quad (40)$$

Taking the concentrations of the reaction products $[Fum^{2-}]$ and [NADH] to be constant, as would be the case if their

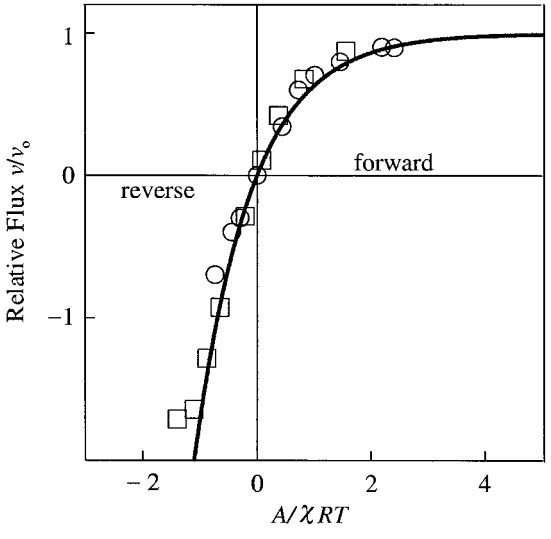

FIGURE 4 Dependence of the relative electron flux v/v_o on thermodynamic drive. Data points (○, □) are relative electron fluxes at various drives observed in experiments (Rottenberg and Gutman, 1977, their Fig. 3) in which the proton motive force was varied. Here, v_o is taken as the observed maximum flux, or that extrapolated to infinite drive. The first data set (○) was obtained for [succinate] = 30 mM, [fumarate] = 100 mM, [NADH] = 0.02 mM, and $[NAD^+]$ = 0.1 mM. The second (□) was measured under similar conditions, except $[NAD^+]$ = 1 mM. According to our analysis, v/v_o is equal to the thermodynamic potential factor F_T. The line shows the curve predicted for $\chi = 4$ by Eq. 36, using ΔE and Δp corresponding to experimental conditions, as described in text.

initial concentrations were large compared to the observed extent of reaction, or if their concentrations were maintained invariant by other metabolic functions, their concentrations can be factored into K_D and K_A, respectively. Assuming that reaction orders such as β_D and β_A are unity and that K_D and K_A remain constant, the rate expression reduces to the dual Monod equation,

$$v = v_{max}\left(\frac{[Suc^{2-}]}{K_D + [Suc^{2-}]}\right)\left(\frac{[NAD^+]}{K_A + [NAD^+]}\right) \quad (41)$$

(Bae and Rittmann, 1996). Where the concentration $[NAD^+]$ of the electron acceptor is maintained constant, or to a value much larger than K_A, this expression can be further simplified to give

$$v = v_{max}\left(\frac{[Suc^{2-}]}{K_D + [Suc^{2-}]}\right), \quad (42)$$

which, in mitochondrial kinetics, is known as the saturation equation, and, in microbial kinetics, as the Monod equation (Monod, 1949). Finally, the zero-order equation $v = v_{max}$ follows from taking $[Suc^{2-}]$ to be constant, or much larger than K_D.

Where Reaction 35 cannot be taken to be far from equilibrium, we must include the thermodynamic term to account for reverse electron flow. If the kinetic terms F_D and F_A can be taken to be constant, as in the zero-order equation above, the rate expression (Eq. 39) simplifies to

$$v = v_{max}\left[1 - \exp\left(-\frac{2F\Delta E + 4F\Delta p}{\chi RT}\right)\right]. \quad (43)$$

Hill's equation (Hill, 1977),

$$v = v_{max}\left[1 - \exp\left(-\frac{2F\Delta E + 4F\Delta p}{RT}\right)\right], \quad (44)$$

follows from taking χ to be one. This equation was the first to recognize the net electron flux as the difference between forward and reverse fluxes. It reflects, furthermore, the limited capacity of the respiratory chain to transmit electrons. The equation has been applied within numerical simulations of oxidative phosphorylation (Rohde and Reich, 1980, Bohnensack, 1981; Boork and Wennerstrom, 1984; Cristina and Hernández, 2000). Hill's equation is strictly correct, however, only where each elementary reaction in the overall electrogenic reaction occurs just once, which is not the case for common redox complexes.

Where Reaction 35 is quite close to equilibrium, the thermodynamic drive is small (i.e., $A/\chi RT$ is close to zero) and the TPF in its mathematical limit reduces to $A/\chi RT$. In this case, Eq. 43 can be simplified to give

$$v = L \times A, \quad (45)$$

where the linear coefficient L is $v_{max}/\chi RT$, and A is thermodynamic drive, $2F\Delta E + 4F\Delta p$. This relation corresponds to the linear equation arising from linear nonequilibrium thermodynamics (Rottenberg, 1973, 1979; Caplan and Essig, 1983; Westerhoff and van Dam, 1987), which predicts that electron flux varies proportionally with thermodynamic drive. Because with increasing drive, the predicted flux increases without bound even though the respiratory chain, in reality, has a limited capacity to transfer electrons, the applicability of this equation is necessarily limited to near-equilibrium conditions.

Thermodynamic control

An increase in the thermodynamic drive across the respiratory chain increases the difference between the activation energies for forward and reverse electron transfer, which, in turn, increases the difference between the forward and reverse electron fluxes. A decrease in drive reduces this difference, ultimately reversing the net flux. Our rate expression expresses the thermodynamic control as the TPF, which can vary from $-\infty$ to 1. Net electron flow proceeds forward where the TPF is positive, and backward where negative; at a TPF of zero, the forward and reverse flows are in balance and there is no net flow.

Thermodynamic drive can be observed in the laboratory by adding phosphate ions to an experiment. The free phosphate changes the phosphorylation potential, altering the PMF. In an experiment in which F_D and F_A can be taken to be constant, the flux capacity v_o is fixed, and the thermodynamic drive F_T is simply given by the relative electron flux v/v_o (Eq. 34). Figure 4 shows the result of two such experiments, conducted by Rottenberg and Gutman (1977, their Fig. 4) for Reaction 35.

In the experiments, the concentrations of all chemical species involved in Reaction 35, except those of the protons, are reported and remain constant, allowing the redox potential to be calculated according to Eq. 10; ΔE is ~ -313 mV in the first set (○), and -285 mV in the second (□). We can determine the PMF, furthermore, from the reported concentrations of ATP, ADP, and P_i, which sets the phosphorylation potential and, assuming equilibrium across F_0F_1–ATP synthase, Δp over the course of the experiments. The only unknown parameter required to evaluate v/v_o according to Eq. 36 is the average stoichiometric number χ, which determines the shape of the curve. As can be seen, if χ is taken to be 4, the thermodynamic drive predicted by our analysis follows the experimental observations closely.

The thermodynamic effect can also be observed by adding an ionophore such as valinomycin or gramicidin to an experiment and observing the electron flux. The ionophore affects the thermodynamic drive by changing the permeability of the cell membrane, altering the electrical potential $\Delta\psi$. In state 3 of mitochondrial respiration, the relative flux v/v_o, a measure of the TPF, follows a negative linear trend with $\Delta\psi$ when the $\Delta\psi$ is greater than $\sim$150 mV (Fig. 5). This trend arises because the electrical potential approxi-

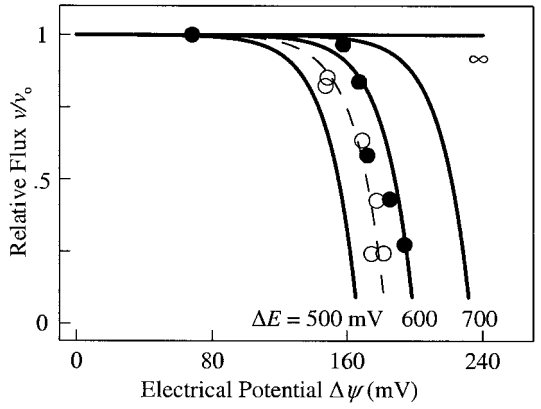

FIGURE 5 Dependence on electrical potential $\Delta\psi$ of relative electron flux v/v_o through the mitochondrial respiratory chain. Data points (○, ●) are values measured at varying $\Delta\psi$ (Lionetti et al., 1996; Murphy and Brand, 1987, respectively), reported as the ratio of measured electron flux to the observed or extrapolated maximum value. Lines show predicted trends calculated using Eq. 20 for various redox potentials ΔE, assuming $n = 2$, $m = 4$, and $\chi = 4$, and taking Δp to be equal to $\Delta\psi$.

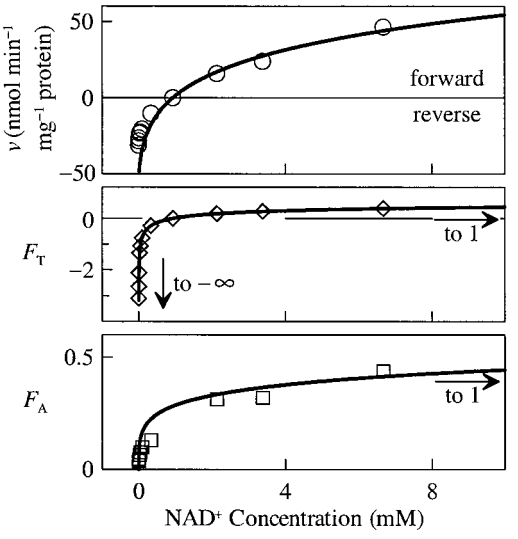

FIGURE 6 Effect of substrate concentration [NAD^+] on electron flow through the mitochondrial respiratory chain during succinate oxidation to NAD^+. Values v are electron fluxes determined experimentally by Rottenberg and Gutman (1977, their Fig. 6). Corresponding TPF values F_T are calculated as in Fig. 4 from experimental conditions, using Eq. 36 with χ of 4. F_A is given by the ratio of v to the product of F_T and the extrapolated maximum electron flux. In their experiment, concentrations of chemical species except NAD^+ remain constant: [succinate] = 30 mM, [fumarate] = 100 mM, [NADH] = 0.02 mM, [ATP] = 1 mM, [ADP] = 0.5 mM, and [P_i] = 0.2 mM. Fluxes are positive for NAD^+ reduction and negative for NADH oxidation. Lines show v, F_T, and F_A as predicted by Eqs. 34, 36, and 38, respectively. According to Eq. 26, F_D remains constant because concentrations of both fumarate and succinate remain constant.

mately counterbalances the redox potential (Eq. 20), leaving little thermodynamic drive. At small drive, as already discussed, the TPF varies linearly with drive, and hence, in this case, with $\Delta\psi$. At electrical potentials considerably less than 150 mV, the relative flux is invariant (Murphy and Brand, 1987; Lionetti et al., 1996) because $\Delta\psi$ is too small to affect the TPF significantly. This transition in behavior has been explained as a shift in the rate-determining step or the loss of thermodynamic control (e.g., Nicholls and Bernson, 1977). Our analysis, in contrast, predicts this result (as shown in Fig. 5) without calling on a change in reaction mechanism.

Effect of substrate concentration

A hyperbolic dependence of electron flux on substrate concentration has been widely observed in experimental studies of mitochondrial (Brown et al., 1990; Gnaiger et al., 1995, 1998, 2000) and microbial respiration (Monod, 1949). Varying substrate concentration changes the redox potential, altering the thermodynamic drive. Where substrate concentration is large, the redox potential is high and the TPF in our model, according to Eq. 20, may approach unity. At small substrate concentrations, the redox potential may be low enough to turn the TPF negative, reversing the electron flow. As a result, the TPF follows a near-hyperbolic trend with substrate concentration (Fig. 6).

Substrate concentration affects not only the thermodynamic drive, but the kinetic controls (F_D and F_A) on electron flux. F_D and F_A also display a hyperbolic dependence on substrate concentration, as shown in Fig. 6. By Eq. 34, we see that the overall hyperbolic dependence of electron flux on substrate concentration arises from the superposition of thermodynamic and kinetic effects. The kinetic factors F_D and F_A are always greater than zero, but the net flux may be negative or positive, depending on the value of the TPF.

These predictions are borne out by electron fluxes observed for Reaction 34 by Rottenberg and Gutman (1977, their Fig. 6), as shown in Fig. 6. In their experiments, the NAD^+ concentration varies, but the concentrations of other chemical species remain constant. We can determine the TPF (i.e., F_T) from the experimental conditions using Eq. 36, taking χ to be 4, as we have done previously (Fig. 4). To calculate v from Eq. 39, we need to determine the unknown parameters k_o (which is v_{max} per mg protein), K_A, and β_A by matching the observed fluxes. Best-fit values for these variables, determined by trial-and-error, are 110 nmol e^-/min/mg protein, 2.5, and 0.3, respectively. Taking note of the fact the F_D remains constant, because the fumarate and succinate concentrations in the experiments are invariant, the kinetic factor F_A can be calculated directly from v and F_T. We see (Fig. 6) that the overall hyperbolic behavior is the superposition of thermodynamic and kinetic effects.

In classic analysis, rate laws such as the Michaelis–Menten equation are derived from enzyme kinetics, and the hyperbolic dependence of rate on substrate concentration

reflects binding between substrate and an enzyme. In our analysis, however, hyperbolic behavior arises from accounting for the conservation of electron carriers. For example, if the concentration of an electron acceptor is raised from a small initial value, the concentration of the oxidized electron carrier $c2^+$ also rises (Eq. 27), increasing the electron flux. With continued increase in electron acceptor concentration, $[c2^+]$ is eventually limited by the size of the pool of electron carrier in the membrane, leading to the observed hyperbolic behavior.

Product inhibition

Reaction products, as they accumulate, can be expected to retard the electron flux, although this effect has received relatively little attention in bioenergetics (Zharova and Vinogradov, 1997; Teusink and Westerhoff, 2000). According to our rate expression, the accumulation of metabolic products should retard the electron flux by decreasing the flux capacity (Eqs. 26 and 27), and by lowering the redox potential ΔE, and hence the TPF (Eq. 21). Figure 7 shows how, in the experimental study of Reaction 34 by Rottenberg and Gutman (1977, their Fig. 5), and according to our analysis, product concentration affects the rate of electron transfer.

In the set of experiments, only fumarate concentration varies. The TPF F_T can be calculated from the experimental conditions, as in Fig. 6. We determined the unknown parameters k_o, K_D, and β_{D^+} required to evaluate the electron flux by Eq. 39 as described previously; best-fit values are 235 nmol e^-/min/mg protein, 1, and 0.5, respectively. The kinetic factor F_D can be calculated directly from v and F_T, because NAD^+ and NADH concentrations are invariant, fixing F_A. As before, the overall effect of product accumulation can be seen in Fig. 7 to be a superposition of kinetic and thermodynamic factors.

Generality of the rate expression

The new rate expression (Eq. 34) is notable in that it accounts rigorously for both kinetic and thermodynamic effects, each of which is necessary to describe the electron flux fully (e.g., Nicholls, 1993). It is the superposition of these terms that controls the overall rate, i.e., the flux varies according to the product of the kinetic and thermodynamic factors.

Because the rate expression integrates thermodynamic and kinetic controls, it offers considerable potential for predicting reaction rates over a range of chemical conditions. Figure 8 shows, for Reaction 35, the relationship between electron fluxes observed in seven sets of experiments reported by Rottenberg and Gutman (1977, their Figs. 4, 5, 6, and 9) and those predicted by the rate expression (Eq. 39). The experiments were conducted under differing conditions, such as changing phosphorylation potential, or varying substrate or product concentration. In calculating the theoretical rates, as we did in preparing Figs. 6 and 7, we took β_D and β_{D^+} to be 0.5, and β_A and β_{A^-} as 0.3; K_D and K_A were set to values of 1 and 2.5. The value of the rate constant k_o can be expected to vary among experiments, because the amount of active mitochondria per mass protein resulting from the preparation technique cannot be controlled well. We used for each set of experiments a single value for k_o in the range 11.6 to 400 nmol e^-/min/mg protein. As can be seen (Fig. 8), the rate expression (Eq. 39) successfully predicts the observed direction and rate of electron transfer for each of the 59 observations.

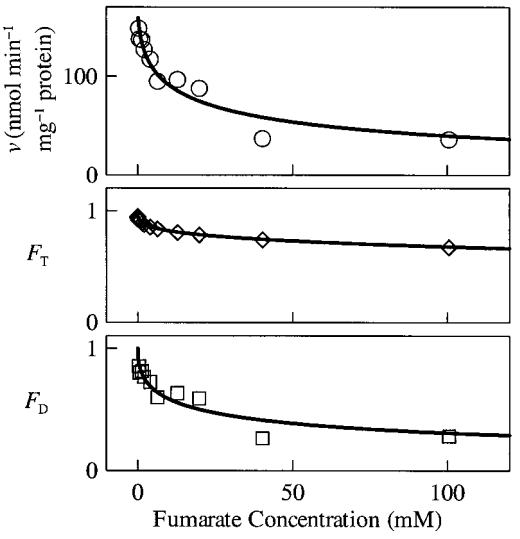

FIGURE 7 Product inhibition of electron flux by fumarate. Values of v are fluxes determined experimentally by Rottenberg and Gutman (1977, their Fig. 5). Corresponding TPF values are calculated, as shown in Fig. 4, from experimental conditions using Eq. 36, taking χ to be 4. F_D is the ratio of v to the product of TPF and extrapolated maximum electron flux. In the experiments, the concentrations of each chemical species except fumarate remain constant: [succinate] = 20 mM, $[NAD^+]$ = 1 mM, [NADH] = 0.1 mM, [ATP] = 1 mM, [ADP] = 0.5 mM, and $[P_i]$ = 0.2 mM. Lines show TPF, F_D, and v as predicted by our models (Eqs. 36, 37, and 34, respectively). According to Eq. 27, F_A remains constant because concentrations of both fumarate and succinate remain constant.

Respiration under alkaline conditions

Our rate expression (Eq. 34), due to its generality, can be used to better understand respiration under conditions that have yet to be studied thoroughly in the laboratory. We consider, as an example, microbial respiration in highly alkaline geochemical environments, such as desert lakes and soils. Where pH falls above ~9, the low proton concentration in the environment makes it difficult for a microbe to maintain a proton motive force across its mem-

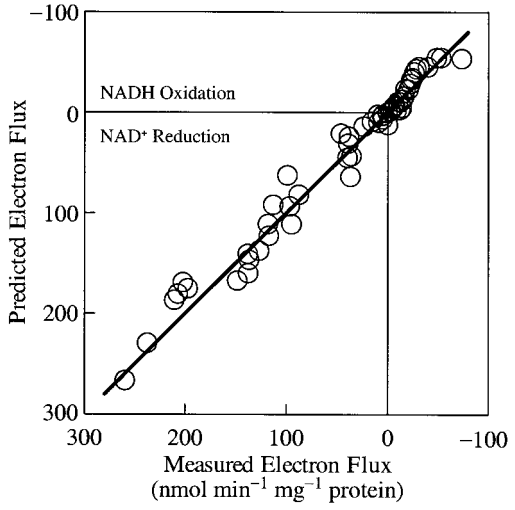

FIGURE 8 Comparison of measured and predicted electron fluxes through mitochondria for NAD^+ reduction by succinate, from seven sets of experiments conducted by Rottenberg and Gutman (1977). Predicted fluxes were calculated by the rate expression (Eq. 39) using the parameter values described in the text and the concentrations of chemical species in Reaction 35, as reported for each set of experiments. The ranges of these concentrations are: [succinate], 2–30 mM; [NAD^+], 0.003–5 mM; [fumarate], 0.033–100 mM; [NADH], 0.02–7 mM; [ATP], 1 mM; [ADP], 0.5 mM; and [P_i], 0.2 or 20 mM.

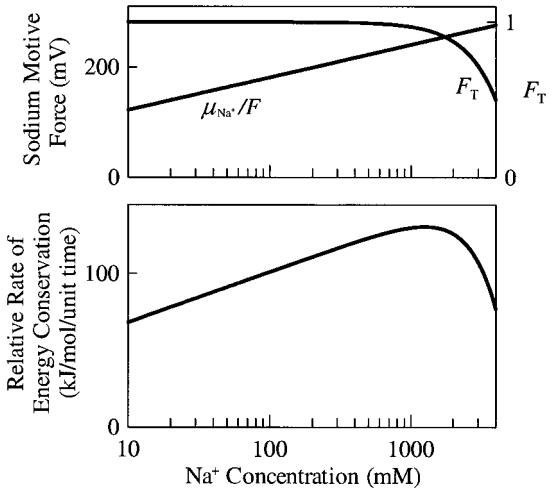

FIGURE 9 Dependence of the sodium motive force, TPF, and relative energy conservation rate on environmental sodium concentration in a hypothetical transport chain that uses sodium as a chemiosmotic ion. Considering a chain that uses NADH as electron donor and oxygen as acceptor, we take $\Delta E = 1140$ mV, $n = 2$, $m = 8$, and $\chi = 4$. We set electrical potential $\Delta\psi$ to 140 mV and sodium concentration inside the membrane to 20 mM. The sodium motive force is given by Eq. 46, and F_T by Eq. 47; the relative conservation rate is the product of F_T, sodium motive force, and m/n.

brane, effectively lowering the PMF by 60–120 mV (Krulwich and Guffanti, 1986).

Some microbes have adapted to alkaline environments by creating a transmembrane electrical potential using sodium ions, rather than protons (White, 1995). They use this potential for metabolic functions such as synthesizing ATP. The sodium motive force μ_{Na^+}/F is

$$\frac{\mu_{Na^+}}{F} = \Delta\psi + \frac{RT}{F}\ln\frac{[Na^+_{out}]}{[Na^+_{in}]}, \qquad (46)$$

where Na^+_{in} and Na^+_{out} refer to sodium ions inside and outside the membrane. The expression for the TPF becomes

$$F_T = 1 - \exp\left(-\frac{nF\Delta E - mF\Delta\psi}{\chi RT}\right)\left(\frac{[Na^+_{out}]}{[Na^+_{in}]}\right)^{m/\chi}, \qquad (47)$$

as can be shown by replacing Δp in Eq. 20 with μ_{Na^+}/F.

Figure 9 shows, for a hypothetical transport chain, how the sodium motive force and TPF vary according to theory as a function of sodium concentration in the environment. Assuming a given concentration of sodium ions inside the membrane, the sodium motive force increases with environmental sodium concentration, as can be seen in Eq. 46. The TPF, ~1 at small sodium concentration, decreases with increasing concentration until it reaches zero where the electrogenic reaction is in equilibrium.

A microbe gains a competitive advantage by maximizing its rate of energy conservation, which is the product of the electron transfer rate v, the sodium motive force μ_{Na^+}/F, and the number of sodium ions translocated per electron, m/n. Figure 9 shows how the relative energy conservation rate ($v/v_o \times$ sodium motive force $\times\ m/n$) in this hypothetical case varies with the environmental sodium concentration. At low salinity, the sodium motive force is small, which maximizes the TPF and electron flux, but decreases the rate of energy conservation. The conservation rate increases with increasing sodium concentration until it reaches a maximum. At higher salinity, the high sodium motive force slows electron transfer by decreasing the thermodynamic drive, causing the energy conservation rate to diminish until, at the electrogenic reaction's equilibrium point, it reaches zero.

The salinity at which a microbe can most rapidly conserve energy depends on the details of the respiratory chain, such as the ratio m/n. In the case shown, this salinity is ~1–2 molal, which is a concentration typical of highly evaporated waters. The analysis shows how the nature of the electron transport chain may affect a microbe's ability to adapt to a certain chemical environment, so that a sodium-translocating microorganism can become adapted to a specific range in salinity.

CONCLUSIONS

We have demonstrated here for the first time that the theory of nonlinear nonequilibrium thermodynamics can be applied to quantify the rate of electron flow through the transport chain of respiring organisms. The theory, which

accounts for both forward and reverse electron flow, leads to a new rate expression that predicts electron flux under arbitrary chemical conditions and varying thermodynamic drive and proton motive force. The rate expression is composed of three terms: one describing kinetic effects attributable to the electron-donating reaction, one for effects of the accepting reaction, and a third term that accounts for the thermodynamic drive. The electron flux varies according to the product of these terms.

The new expression differs from previously proposed relationships in its generality. Written in general form, it appears complex. Once the specific forms of the donating and accepting reactions are specified, however, it simplifies readily to a more manageable equation. The equation can be further simplified under certain chemical conditions or thermodynamic states to give rate laws of forms familiar in cellular physiology and microbial ecology.

The rate expression correctly predicts the widely observed nonlinear dependence of electron flux on PMF and reveals that the relationship between electron flux and substrate concentration results from superposition of a near-hyperbolic effect of concentration on the TPF, and a hyperbolic effect on the flux capacity. It demonstrates the nature of the inhibiting effects of reaction products, and successfully predicts experimentally determined directions and rates of electron transfer through the respiratory chain. The generality of this expression offers new understanding of the controls on cell respiration rates, and the potential for predicting respiration rates over broader ranges of conditions than has been possible to date.

APPENDIX: STEP D OR A CONSUMES THERMODYNAMIC DRIVE

Rate expressions parallel to Eq. 34 can be derived for the cases in which the electron-donating or -accepting step (D or A), instead of the electron transfer step (T), consumes most of the thermodynamic drive. For the case of step D, v_o is given by the form of Reaction 4 to be

$$v_o = k_+[\mathrm{E_D}] \prod_\mathrm{D} [\mathrm{D}]^{\alpha_\mathrm{D}}[\mathrm{c1}^+]. \tag{A1}$$

Here, $\mathrm{E_D}$ is the redox complex catalyzing step D, and α_D is the reaction order. A factor ξ_D gives the ratio of redox complex concentration $[\mathrm{E_D}]$ to protein mass or total biomass [X].

Taking the thermodynamic drives for steps T and A to be negligible, the ratio in concentration of carrier 1 in oxidized to reduced forms is

$$\frac{[\mathrm{c1}^+]}{[\mathrm{c1}]} = \frac{\prod_\mathrm{A} [\mathrm{A}]^{\beta_\mathrm{A}}}{K_\mathrm{A} \prod_\mathrm{A} [\mathrm{A}^-]^{\beta_{\mathrm{A}^-}}}, \tag{A2}$$

where

$$\beta_\mathrm{A} = \frac{\nu_\mathrm{A}}{\nu_{\mathrm{c1}}} \quad \text{and} \quad \beta_{\mathrm{A}^-} = \frac{\nu_{\mathrm{A}^-}}{\nu_{\mathrm{c1}}} \tag{A3}$$

and

$$K_\mathrm{A} = \exp\left[- \frac{nF(\Delta E^\circ_\mathrm{T} + \Delta E^\circ_\mathrm{A}) - (m_\mathrm{T} + m_\mathrm{A})F\Delta p}{\nu_{\mathrm{c1}} RT} \right]. \tag{A4}$$

Here, $\Delta E^\circ_\mathrm{T}$ is the standard redox potential difference of Reaction 5.

Combining Eqs. A2 and A4 with mass balance for the electron carrier gives

$$F_\mathrm{A} = \frac{[\mathrm{c1}^+]}{[\mathrm{c1}]_\mathrm{t}} = \frac{\prod_\mathrm{A} [\mathrm{A}]^{\beta_\mathrm{A}}}{\prod_\mathrm{A} [\mathrm{A}]^{\beta_\mathrm{A}} + K_\mathrm{A} \prod_{\mathrm{A}^-} [\mathrm{A}^-]^{\beta_{\mathrm{A}^-}}}. \tag{A5}$$

Now,

$$k_\mathrm{o} = k_+ \xi_\mathrm{D} [\mathrm{c1}]_\mathrm{t}, \tag{A6}$$

and the final rate expression is

$$v = \nu_{\max} \left(\prod_\mathrm{D} [\mathrm{D}]^{\alpha_\mathrm{D}} \right) F_\mathrm{A} F_\mathrm{T}. \tag{A7}$$

Similarly, if step A consumes most of the drive, the rate expression becomes

$$v = \nu_{\max} F_\mathrm{D} \left(\prod_\mathrm{A} [\mathrm{A}]^{\alpha_\mathrm{A}} \right) F_\mathrm{T}, \tag{A8}$$

where

$$k_\mathrm{o} = k_+ \xi_\mathrm{A} [\mathrm{c2}]_\mathrm{t} \tag{A9}$$

and

$$K_\mathrm{D} = \exp\left[- \frac{nF(\Delta E^\circ_\mathrm{D} + \Delta E^\circ_\mathrm{T}) - (m_\mathrm{D} + m_\mathrm{T})F\Delta p}{\nu_{\mathrm{c2}} RT} \right]. \tag{A10}$$

As before, these equations simplify immediately when applied to a given combination of donating and accepting reactions, and under specific chemical conditions.

We thank Robert Blankenship, Bernard Korzeniewski, James Imlay, Thomas Johnson, Robert Sanford, and two anonymous reviewers for their interest and generous advice.

This work was supported by the research sponsors of the Hydrogeology Program: Chevron, ExxonMobil Upstream Research, Idaho National Engineering and Environmental Laboratory, Lawrence Livermore, Sandia, SCK-CEN, Texaco, and the United States Geological Survey.

REFERENCES

Bae, W., and B. E. Rittmann. 1996. A structured model of dual-limitation kinetics. *Biotechnol. Bioeng.* 49:683–689.

Bohnensack, R. 1981. Control of energy transformation of mitochondria. Analysis by a quantitative model. *Biochim. Biophys. Acta.* 634:203–218.

Boork, J., and H. Wennerstrom. 1984. The influence of membrane potentials on reaction rates. Control in free-energy-transducing systems. *Biochim. Biophys. Acta.* 767:314–320.

Boudart, M. 1976. Consistency between kinetics and thermodynamics. *J. Phys. Chem.* 80:2869–2870.

Brown, G. C. 1992. Control of respiration and ATP synthesis in mammalian mitochondria and cells. *Biochem. J.* 284:1–13.

Brown, G. C., P. L. Lakin-Thomas, and M. D. Brand. 1990. Control of respiration and oxidative phosphorylation in isolated rat liver cells. *Eur. J. Biochem.* 192:355–362.

Caplan, S. R., and A. Essig. 1983. Bioenergetics and Linear Nonequilibrium Thermodynamics: the Steady State. Cambridge, Massachusetts: Harvard University Press.

Christensen, H. N. 1975. Biological Transport. Reading, Massachusetts: W.A. Benjamin, Inc. 63–106.

Cristina, E., and J. A. Hernández. 2000. An elementary kinetic model of energy coupling in biological membranes. *Biochim. Biophys. Acta.* 1460:276–290.

Davidson, V. L. 1996. Unraveling the kinetic complexity of interprotein electron transfer reactions. *Biochemistry.* 35:14035–14039.

De Donder, T. H., and P. Van Pysselberghe. 1936. Thermodynamic Theory of Affinity. Stanford, California: Stanford University Press. 30–41.

Fell, D. A. 1992. Metabolic control analysis: a survey of its theoretical and experimental development. *Biochem. J.* 286:313–330.

Gnaiger, E., B. Lassnig, A. V. Kuznetsov, and R. Margreiter. 1998. Mitochondrial respiration in the low oxygen environment of the cell. Effect of ADP on oxygen kinetics. *Biochim. Biophys. Acta.* 1365: 249–254.

Gnaiger, E., G. Méndez, and S. C. Hand. 2000. High phosphorylation efficiency and depression of uncoupled respiration in mitochondria under hypoxia. *Proc. Natl. Acad. Sci. U.S.A.* 97:11080–110805.

Gnaiger, E., R. Steinlechner-Maran, G. Mendez, T. Eberl, and R. Margreiter. 1995. Control of mitochondrial and cellular respiration by oxygen. *J. Bioenerg. Biomembr.* 27:583–596.

Groen, A. K., R. J. Wanders, H. V. Westerhoff, R. van der Meer, and J. M. Tager. 1982. Quantification of the contribution of various steps to the control of mitochondrial respiration. *J. Biol. Chem.* 257:2754–2757.

Happel, J. 1972. Study of kinetic structure using marked atoms. *Catal. Rev.* 6:221–260.

Hill, T. L. 1977. Free Energy Transduction in Biology: The Steady-State Kinetics and Thermodynamic Formalism. New York: Academic Press. 33–56.

Hollingsworth, C. A. 1957. Kinetics and equilibria of complex reactions. *J. Chem. Phys.* 27:1346–1348.

Holzhütter, H.-G., W. Henke, W. Dubiel, and G. Gerber. 1985. A mathematical model to study short-term regulation of mitochondrial energy transduction. *Biochim. Biophys. Acta.* 810:252–268.

Horiuti, J. 1948. A method of statistical mechanical treatment of equilibrium and chemical reactions. *J. Res. Inst. Catal. Hokkaido Univ.* 1:8–79.

Kacser, K., and J. A. Burns. 1979. Molecular democracy: who shares the controls? *Biochem. Soc. Trans.* 7:1150–1160.

Korzeniewski, B., and W. Froncisz. 1991. An extended dynamic model of oxidative phosphorylation. *Biochim. Biophys. Acta.* 1060:210–223.

Korzeniewski, B., and J.-P. Mazat. 1996. Theoretical studies on the control of oxidative phosphorylation in muscle mitochondria: application to mitochondrial deficiencies. *Biochem. J.* 319:143–148.

Krulwich, T. A., and A. A. Guffanti. 1986. Regulation of internal pH in acidophilic and alkalophilic bacteria. *Methods Enzymol.* 125:352–365.

Lionetti, L., S. Iossa, M. D. Brand, and G. Liverini. 1996. Relationship between membrane potential and respiration rate in isolated liver mitochondria from rats fed an energy dense diet. *Mol. Cell. Biochem.* 158:133–138.

Masel, R. I. 2001. Chemical Kinetics and Catalysis. New York: Wiley-Interscience. 25–26.

Mitchell, P. 1961. Coupling of phosphorylation to electron and hydrogen transfer by a chemiosmotic type of mechanism. *Nature.* 191:144–148.

Mitchell, P. 1966. Chemiosmotic coupling in oxidative and photosynthetic phosphorylation. *Biol. Rev. Camb. Philos. Soc.* 41:445–502.

Mitchell, P. 1968. Chemiosmotic Coupling and Energy Transduction. Bodmin, Cornwall, U.K.: Glynn Research, Ltd. 1–111.

Monod, J. 1949. The growth of bacterial cultures. *Annu. Rev. Microbiol.* 3:364–371.

Moreno-Sánchez, R., C. Bravo, and H. V. Westerhoff. 1999. Determining and understanding the control of flux. An illustration in submitochondrial particles of how to validate schemes of metabolic control. *Eur. J. Biochem.* 264:427–433.

Murphy, M. P., and M. D. Brand. 1987. The control of electron flux through cytochrome oxidase. *Biochem. J.* 243:499–505.

Nicholls, D. G., and V. S. Bernson. 1977. Inter-relationships between proton electrochemical gradient, adenine-nucleotide phosphorylation potential and respiration, during substrate-level and oxidative phosphorylation by mitochondria from brown adipose tissue of cold-adapted guinea-pigs. *Eur. J. Biochem.* 75:601–612.

Nicholls, P. 1993. Control of cytochrome *c* oxidase: kinetic, thermodynamic or allosteric? In: Modern Trends in Biothermokinetics. S. Schuster, M. Rigoulet, R. Ouhabi, and J. P. Mazat, editors. New York: Plenum. 11–16.

Price, G. 1998. Thermodynamics of Chemical Processes. New York: Oxford University Press. 39–62.

Pring, M. 1969. The analysis of electron transport kinetics in mitochondria. In: Concepts and Models of Biomathematics: Simulation Techniques and Methods. F. Heinmetz, editor. New York: Dekker. 75–104.

Richardson, D. J. 2000. Bacterial respiration: a flexible process for a changing environment. *Microbiology.* 146:551–571.

Rohde, K., and J. G. Reich. 1980. Theoretical study of an energy metabolizing system satisfying Mitchell's postulates. *Acta Biol. Med. Ger.* 39:367–380.

Rottenberg, H. 1973. The thermodynamic description of enzyme-catalyzed reactions. The linear relation between the reaction rate and the affinity. *Biophys. J.* 13:503–511.

Rottenberg, H. 1979. Non-equilibrium thermodynamics of energy conversion in bioenergetics. *Biochim. Biophys. Acta.* 549:225–253.

Rottenberg, H., and M. Gutman. 1977. Control of the rate of reverse electron transport in submitochondrial particles by the free energy. *Biochemistry.* 16:3220–3227.

Temkin, M. I. 1963. Kinetics of stationary reactions. *Dokl. Akad. Nauk SSSR* 152:156–159.

Teusink, B., and H. V. Westerhoff. 2000. "Slave" metabolites and enzymes. A rapid way of delineating metabolic control. *Eur. J. Biochem.* 267:1889–1893.

Westerhoff, H. V., and K. van Dam. 1987. Thermodynamics and Control of Biological Free-energy Transduction. Amsterdam: Elsevier. 213–290.

White, D. 1995. The Physiology and Biochemistry of Prokaryotes. New York: Oxford University Press. 53–55.

Wilson, D. F., C. S. Owen, and M. Erecinska. 1979. Quantitative dependence of mitochondrial oxidative phosphorylation on oxygen concentration: a mathematical model. *Arch. Biochem. Biophys.* 195: 494–504.

Wilson, D. F., C. S. Owen, and A. Holian. 1977. Control of mitochondrial respiration: a quantitative evaluation of the roles of cytochrome *c* and oxygen. *Arch. Biochem. Biophys.* 182:749–762.

Zharova, T. V., and A. D. Vinogradov. 1997. A competitive inhibition of the mitochondrial NADH-ubiquinone oxidoreductase (Complex I) by ADP-ribose. *Biochim. Biophys. Acta.* 1320:256–264.